Title	Analysis approach of SSO based on LDAE model
Author(s)	Yu, C; Ni, Y
Citation	The 15th Power Systems Computation Conference (PSCC'05), Liège, Belgium, 22-26 August 2005. In Proceedings of 15th PSCC, 2005, p. 1-7
Issued Date	2005
URL	http://hdl.handle.net/10722/99288
Rights	This work is licensed under a Creative Commons Attribution-NonCommercial-NoDerivatives 4.0 International License.

ANALYSIS APPROACHES OF SSO BASED ON LDAE MODEL

Chang Yu, and Yixin Ni, *Senior Member, IEEE*
The University of Hong Kong
Hong Kong, China
changyu@eee.hku.hk

Abstract – A linearized differential and algebraic equations (LDAE) model for both eigen-analysis and complex torque coefficient (CTC) calculation of power system subsynchronous oscillation (SSO) is proposed in this paper. The LDAE model for SSO study is derived at first. Generalized eigen-analysis and CTC calculation based on the LDAE model are presented thereafter. The effectiveness of the proposed LDAE model based SSO analysis approaches are verified through computer test results. The LDAE-model-based SSO study approach suggested in this paper paves the way for SSO study with HVDC transmission and/or FACTS devices without eliminating their algebraic variables, which can obtain more valuable information.

Keywords: SSO, Complex torque coefficient, Generalized eigenvalue, LDAE

1 INTRODUCTION

Subsynchronous Oscillation (SSO) is a complex stability issue in power systems and there have been a lot of research outputs on SSO in recent decades [1]. The preliminary studies on SSO concerned mainly about induction generator effect induced by series compensation capacitor. In early 1970s, series compensation stimulated electromechanical torsional interaction, which caused severe torsional oscillations and damage of turbine-generator shafts, attracted great attention and research work. This led to a new period of SSO study. In late 1970's, HVDC transmission system caused SSO was first observed and brought about in-depth studies on device-dependent SSO. The application of FACTS technology has promoted the study on device-dependent SSO even more significantly [2~4].

In order to study SSO, various methods are used [5, 6]. Among them time simulation is the most direct way, in which EMT models of power system elements with multi-mass spring shaft effects and step-by-step numerical integration methods are used to get time-evolution of various variables in SSO. A distinct advantage of time simulation method is that it allows detailed modeling of power system elements with system nonlinearity included. Therefore it is very useful for the study of transient torque amplifying effect and the examination of SSO damping control performance under large disturbances. However, using EMT models for SSO study is time consuming for its extremely small time step especially when there are HVDC transmission and/or FACTS devices in the studied power system. Besides, time simulation is poor in physical transparency and difficult to reveal SSO principles. Small signal stability study is another method widely used for SSO study, where the power system model is linearized around the system operation point and converted to a standard form of $\dot{\boldsymbol{x}} = \boldsymbol{A_S x}$ ($\boldsymbol{A}_S$ is the system state-space matrix). Eigen-analysis is then conducted to get deep in-sight of system SSO characteristics. Eigen-analysis is an accurate method which can examine the effects of system control and parameters on damping the torsional modal oscillation. With the help of mature linear control theories, advanced SSO damping control can be realized. However, in a real power system with HVDC transmission and/or FACTS devices, it is time-consuming in deriving system matrix $\boldsymbol{A}_S$ with all the algebraic variables eliminated. Moreover, after reduction of algebraic variables, it may be inconvenient to conduct certain eigenvalue sensitivity analysis based on $\boldsymbol{A}_S$. When the studied power system is rather complicated with higher orders, both time simulation and eigen-analysis methods may have difficulties in analysis without system reduction. In recent years frequency-scanning based methods become computationally attractive because they can provide system damping information over the entire subsynchronous frequency band [7], although they might not be so precise as eigen-analysis method. Among them the complex torque coefficient (CTC) method (or say torque per unit speed method) is most suitable to large-scale power system SSO analysis with the capability of showing clearly the system electric damping effects over SSO frequency band.

In this paper, a linearized differential and algebraic equations (LDAE) model for both eigen-analysis and CTC calculation of SSO is proposed. In the LDAE approach, the LDAEs of individual power system components are derived first, which act as building blocks of overall system model. The system model can then be established quickly and easily according to the network topology. This method is very suitable for SSO study of power systems with HVDC transmission and/or FACTS devices without the need of eliminating their algebraic variables. Generalized eigen-analysis technique [8] can be directly applied to the LDAE model. The results can provide useful information of observability and controllability of algebraic variables on individual SSO modes, which is very useful in control design. Furthermore, the frequency-scanning CTC analysis method can be easily realized base on the LDAE model. The stability of torsional modes based on their damping torque coefficients is also discussed. The effectiveness of the proposed LDAE model and the relevant analysis approaches is verified with computer test results. The LDAE-based SSO study model and its corresponding analysis approaches pave the way to include HVDC transmission and FACTS device models in SSO study and get deep insight about their effects on SSO.

The paper is arranged as follows. The LDAE model for SSO is derived in section 2. The LDAE-model-based generalized eigen-analysis for SSO is presented in section 3. The CTC calculation method based on the LDAE model is described in section 4. Finally computer test results are given in section 5 with conclusions drawn in section 6.

2 LDAE MODEL FOR SSO STUDY

Power systems can be expressed by a set of nonlinear differential and algebraic equations (DAE):

$$\begin{cases} \dot{\boldsymbol{x}} = \boldsymbol{f(x, y)} \\ \boldsymbol{0} = \boldsymbol{g(x, y)} \end{cases}$$

where $\boldsymbol{x}$: the vector of state variables; $\boldsymbol{y}$: the vector of algebraic variables.

Linearizing the above equations around the operation point, we have:

$$\begin{cases} \Delta\dot{\boldsymbol{x}} = \boldsymbol{A}\Delta\boldsymbol{x} + \boldsymbol{B}\Delta\boldsymbol{y} \\ \boldsymbol{0} = \boldsymbol{C}\Delta\boldsymbol{x} + \boldsymbol{D}\Delta\boldsymbol{y} \end{cases} \quad (1)$$

where $\boldsymbol{A} = \frac{\partial \boldsymbol{f}}{\partial \boldsymbol{x}}$, $\boldsymbol{B} = \frac{\partial \boldsymbol{f}}{\partial \boldsymbol{y}}$, $\boldsymbol{C} = \frac{\partial \boldsymbol{g}}{\partial \boldsymbol{x}}$, $\boldsymbol{D} = \frac{\partial \boldsymbol{g}}{\partial \boldsymbol{y}}$ calculated at the equilibrium point; Δ: an operator to represent perturbed values.

From (1), we can eliminate all algebraic variables $\boldsymbol{y}$ if $\boldsymbol{D}^{-1}$ exists, which leads to linearized ordinary differential equations (LODE) model in state space:

$$\Delta\dot{\boldsymbol{x}} = \boldsymbol{A}_S\Delta\boldsymbol{x} \quad (2)$$

where system matrix $\boldsymbol{A_S} = \boldsymbol{A} - \boldsymbol{BD}^{-1}\boldsymbol{C}$. Equation (2) is widely used for conventional eigen-analysis as mentioned above.

However, to eliminate all the algebraic variables in real power systems with HVDC transmission or/and FACTS devices might be time consuming. Moreover the item of "$\boldsymbol{BD}^{-1}\boldsymbol{C}$" makes $\boldsymbol{A}_S$ unable to be expressed by system parameters explicitly, which, under certain circumstances, increases the difficulty in eigenvalue sensitivity analysis. In this paper, the system sub-matrices $\boldsymbol{A}$, $\boldsymbol{B}$, $\boldsymbol{C}$, $\boldsymbol{D}$ will be kept, and eigen-analysis for SSO study will be based on the system LDAE model (1) directly.

Power system component models for SSO study can be found in [9]. After linearization of component models at operation point, we can get LDAE models with algebraic variables preserved for various components as follows.

Take the turbine shaft system of a synchronous machine as an example. Suppose the shaft of a turbine generator can be expressed as a six-mass spring system, and its LDAE model is ($\boldsymbol{X}$: state variables; $\boldsymbol{Y}$: algebraic variables):

$$\dot{\boldsymbol{X}}_S = \boldsymbol{A}_{SS}\boldsymbol{X}_S + \boldsymbol{B}_{STe}\boldsymbol{Y}_{Te} \quad (3)$$

where $\boldsymbol{X}_S$ = $(\Delta\delta_1 \ldots \Delta\delta_G \ldots \Delta\delta_6\ ,\ \Delta\omega_1 \ldots \Delta\omega_G \ldots \Delta\omega_6)^T$: angle and speed increments of the six-mass shaft; $\boldsymbol{Y}_{Te} = \Delta T_e$: electromagnetic torque of generator mass (For simplicity, the speed governor's dynamics is neglected), which can be expressed as a function of generator winding currents and flux linkages in *d-q* coordinates (in LDAE format):

$$\boldsymbol{0} = \boldsymbol{C}_{TeG}\boldsymbol{X}_G + \boldsymbol{D}_{Tei}\boldsymbol{Y}_i + \boldsymbol{D}_{Te}\boldsymbol{Y}_{Te} \quad (4)$$

where $\boldsymbol{X}_G = (\Delta\psi_d, \Delta\psi_q, \Delta\psi_f, \Delta\psi_D, \Delta\psi_g, \Delta\psi_Q)^T$: generator winding flux linkages in *d-q* coordinates assuming a generator has six windings, $\boldsymbol{X}_G = \boldsymbol{L}_{Gi}\cdot\boldsymbol{Y}_i$ with $\boldsymbol{Y}_i = (\Delta i_d, \Delta i_q, \Delta i_f, \Delta i_D, \Delta i_g, \Delta i_Q)^T$: generator winding currents in *d-q* coordinates. To keep $\boldsymbol{Y}_{Te}$ and (4) explicitly in system model is good for future CTC calculation over subsynchronous frequency range through frequency-scanning.

Similarly, we can obtain LDAEs for electromagnetic circuit of machines, excitation systems, transformers, transmission lines, loads, and shunt capacitors, etc.

In the generator LDAE model, we preserve the algebraic variables of generator terminal voltages and currents in *d-q* coordinates ($\boldsymbol{Y}_u$ & $\boldsymbol{Y}_i$), and their companion variables in *x-y* synchronous coordinates ($\boldsymbol{Y}_u^{(xy)}$ & $\boldsymbol{Y}_i^{(xy)}$). Hence, the algebraic equations for coordinates transformation between *d-q* and *x-y* can be directly included in system model as shown in (5):

$$\begin{bmatrix} \Delta f_d \\ \Delta f_q \end{bmatrix} = \begin{bmatrix} \sin\delta_{G0} & -\cos\delta_{G0} \\ \cos\delta_{G0} & \sin\delta_{G0} \end{bmatrix} \begin{bmatrix} \Delta f_x \\ \Delta f_y \end{bmatrix} + \begin{bmatrix} f_{q0} \\ -f_{d0} \end{bmatrix} \Delta\delta_G \quad (5)$$

where f can be u or i to denote generator terminal voltage or current respectively; δ_G: rotor angle of generator-mass which is the leading angle of its *q*-axis w.r.t. the synchronous coordinate *x*-axis.

Keeping (5) in DAE model is beneficial to fast interface of generator with ac network. Equation (5) for generator terminal voltages and injection currents coordinates transformation can be rewritten to:

$$\begin{cases} \boldsymbol{0} = \boldsymbol{C}_{iS}\boldsymbol{X}_S + \boldsymbol{D}_{ii}\boldsymbol{Y}_i + \boldsymbol{D}_{ii}^{(xy)}\boldsymbol{Y}_i^{(xy)} \\ \boldsymbol{0} = \boldsymbol{C}_{uS}\boldsymbol{X}_S + \boldsymbol{D}_{uu}\boldsymbol{Y}_u + \boldsymbol{D}_{uu}^{(xy)}\boldsymbol{Y}_u^{(xy)} \end{cases} \quad (6)$$

And then according to the network topology, the bus-line incident matrices can be obtained. Assuming $\boldsymbol{C}_{NA}$, $\boldsymbol{C}_{NT}$, $\boldsymbol{C}_{NL}$, $\boldsymbol{D}_{NG}$ and $\boldsymbol{D}_{NC}$ are the incident matrices of network buses w.r.t. transmission lines, transformer branches, load branches, generator branches, and shunt capacitor branches respectively, bus injection current balance equations based on *KCL* will be:

$$\begin{aligned} \boldsymbol{0} = \boldsymbol{C}_{NA}\boldsymbol{X}_A + \boldsymbol{C}_{NT}\boldsymbol{X}_T + \boldsymbol{C}_{NL}\boldsymbol{X}_L \\ + \boldsymbol{D}_{NG}\boldsymbol{Y}_i^{(xy)} + \boldsymbol{D}_{NC}\boldsymbol{Y}_i^{(C)} \end{aligned} \quad (7)$$

where $\boldsymbol{X}_A$: transmission line current; $\boldsymbol{X}_T$: transformer branch current; $\boldsymbol{X}_L$: load branch current; $\boldsymbol{Y}_i^{(xy)}$: generator terminal current; $\boldsymbol{Y}_i^{(C)}$: shunt capacitor branch current.

After combining all the individual LDAEs together, the entire system LDAE model for SSO study takes the form:

$$\begin{bmatrix} \dot{\boldsymbol{X}} \\ \boldsymbol{0} \end{bmatrix} = \begin{bmatrix} \boldsymbol{A} & \boldsymbol{B} \\ \boldsymbol{C} & \boldsymbol{D} \end{bmatrix} \begin{bmatrix} \boldsymbol{X} \\ \boldsymbol{Y} \end{bmatrix} \quad (8)$$

where the algebraic equations include the generator electromagnetic torque computation equations (see (4)); the generator winding flux linkage equations; the coordinates transformation equations for generator currents and voltages (see (5) and (6)); and bus injection current balance equations (see (7)).

A brief discussion on (8) is made as follows.

(i) Matrices $\boldsymbol{A}$, $\boldsymbol{B}$, $\boldsymbol{C}$, and $\boldsymbol{D}$ are extremely sparse. In $\boldsymbol{A}$ and $\boldsymbol{D}$, the non-zero block-matrices are mainly on the diagonal and most of them are also very sparse. Hence sparse matrix techniques can be use to conduct eigen-analysis. The computation work can decrease noticeably, which is significant to SSO study of real power systems.

(ii) The LDAE formulation approach breaks down the modeling issue into two parts, one is element-modeling part and another is network topology and integration part. Therefore, if we want to study the impacts of HVDC transmission and/or FACTS devices on SSO, we can just easily add their individual LDAE models to (8); and then modify the corresponding bus injection current balance equation (7) (to include their injection current effects). The process is simple and direct.

(iii) The advanced generalized eigen-analysis method can be directly applied to the LDAE model. The corresponding generalized eigenvectors can provide very useful information on observability and controllability of both state and algebraic variables w.r.t a certain SSO mode. This is a significant feature of the suggested method, which can provide deep insight into system SSO characteristics and is beneficial to controller design for SSO damping (see section 3 for details).

(iv) The suggested LDAE model formulation can avoid sacrificing the physical structure transparency due to the elimination of algebraic variables in traditional LODE modeling. Since system parameters can be shown explicitly in the LDAE model, it is convenient to make eigenvalue sensitivity analysis w.r.t system parameter perturbation.

(v) Keeping the differential operator $p = d/dt$ in the LDAE model, and then setting $p = j\Omega$ (Ω is in SSO frequency band), we can quickly compute the CTC $\Delta T_e/\Delta\delta_G$ at frequency Ω. So frequency-scanning analysis can be easily performed based on the LDAE model (see section 4 for details).

3 GENERALIZED EIGEN-ANALYSIS BASED ON THE LDAE MODEL

For the traditional eigen-analysis of (8), we usually eliminate algebraic variables $\boldsymbol{Y}$ and get:

$$\dot{\boldsymbol{X}} = \boldsymbol{A}_S \boldsymbol{X} \tag{9}$$

where $\boldsymbol{A}_{S(n\times n)} = \boldsymbol{A} - \boldsymbol{B}\boldsymbol{D}^{-1}\boldsymbol{C}$ assuming $\boldsymbol{D}^{-1}$ exists.

Clearly, $\boldsymbol{A}_S$ might not be sparse. Its physical transparency may be lost due to the elimination of algebraic variables. Eigenvalue and right & left eigenvector computation based on (9) is given in (10):

$$\begin{cases} \det(\lambda \boldsymbol{I} - \boldsymbol{A}_S) = 0 \\ \lambda_i \boldsymbol{e}_i = \boldsymbol{A}_S \boldsymbol{e}_i , \lambda_i \boldsymbol{f}_i = \boldsymbol{A}_S^{\mathrm{T}} \boldsymbol{f}_i \end{cases} \tag{10}$$

where $\boldsymbol{I}$ is identity matrix; $\boldsymbol{e}_i$ and $\boldsymbol{f}_i$ are the right and left eigenvectors with respect to the i^{th} eigenvalue (λ_i) of $\boldsymbol{A}_S$.

For LDAE model (8), we shall conduct generalized eigenvalue and eigenvector calculation using generalized Schur decomposition method [8]. For the suggested LDAE model (8), if we define:

$\boldsymbol{T} = \begin{bmatrix} \boldsymbol{X} \\ \boldsymbol{Y} \end{bmatrix}$; $\widetilde{\boldsymbol{A}} = \begin{bmatrix} \boldsymbol{A} & \boldsymbol{B} \\ \boldsymbol{C} & \boldsymbol{D} \end{bmatrix}$: extended system matrix; $\widetilde{\boldsymbol{H}} = \begin{bmatrix} \boldsymbol{I}_{n\times n} & \boldsymbol{0}_{n\times m} \\ \boldsymbol{0}_{m\times n} & \boldsymbol{0}_{m\times m} \end{bmatrix}$ (where n and m are the number of the state variables in $\boldsymbol{X}$ and the number of the algebraic variables in $\boldsymbol{Y}$), we can rewrite (8) into:

$$\widetilde{\boldsymbol{H}}\dot{\boldsymbol{T}} = \widetilde{\boldsymbol{A}}\boldsymbol{T} \tag{11}$$

The solution of equation (11) is equivalent to solve the generalized eigenvalue problem:

$$\lambda \widetilde{\boldsymbol{H}}\boldsymbol{T} = \widetilde{\boldsymbol{A}}\boldsymbol{T} \tag{12}$$

If $\widetilde{\boldsymbol{H}}$ is nonsingular, we can convert the problem to a standard eigen-problem $(\widetilde{\boldsymbol{H}}^{-1}\widetilde{\boldsymbol{A}})\boldsymbol{T} = \lambda \boldsymbol{T}$ to solve the generalized eigenvalues of (12). However, for our case, $\widetilde{\boldsymbol{H}}$ is singular and $\widetilde{\boldsymbol{H}}^{-1}$ does not exist. An advanced eigenvalue computation technique, i.e. generalized Schur decomposition method [8], is adopted, through which the inverse calculation of $\widetilde{\boldsymbol{H}}$ can be avoided and the original system eigenvalues can be calculated efficiently. Hence this is an ideal method to solve the special generalized eigen-problem with rank-deficient $\widetilde{\boldsymbol{H}}$.

According to generalized Schur decomposition for a pair of complex square matrices ($\widetilde{\boldsymbol{H}}$, $\widetilde{\boldsymbol{A}}$) of same dimension ($l\times l$), it is proven that there exists a pair of unitary matrices $\boldsymbol{Q}_{(l\times l)}$ and $\boldsymbol{Z}_{(l\times l)}$ ($\boldsymbol{Q}\cdot\boldsymbol{Q}^H = \boldsymbol{I}$, $\boldsymbol{Z}\cdot\boldsymbol{Z}^H = \boldsymbol{I}$) such that:

$$\boldsymbol{Q}\widetilde{\boldsymbol{H}}\boldsymbol{Z}^H = \hat{\boldsymbol{H}} \text{ , } \boldsymbol{Q}\widetilde{\boldsymbol{A}}\boldsymbol{Z}^H = \hat{\boldsymbol{A}} \tag{13}$$

where both $\hat{\boldsymbol{H}}$ and $\hat{\boldsymbol{A}}$ are **upper triangular** matrices.

Left-multiplying (12) by $\boldsymbol{Q}$ we have:

$$\lambda \boldsymbol{Q}\widetilde{\boldsymbol{H}}(\boldsymbol{Z}^H\boldsymbol{Z})\boldsymbol{T} = \boldsymbol{Q}\widetilde{\boldsymbol{A}}(\boldsymbol{Z}^H\boldsymbol{Z})\boldsymbol{T} \tag{14}$$

According to (13), equation (14) will be (define $\boldsymbol{T}' = \boldsymbol{Z}\boldsymbol{T}$):

$$\lambda \hat{\boldsymbol{H}}\boldsymbol{T}' = \hat{\boldsymbol{A}}\boldsymbol{T}' \tag{15}$$

Equation (15) is equivalent to solve homogeneous linear equations $(\lambda\hat{\boldsymbol{H}} - \hat{\boldsymbol{A}})\boldsymbol{T}' = \boldsymbol{0}$. The sufficient and necessary condition for the existence of non-zero $\boldsymbol{T}'$ is:

$$\det(\lambda\hat{\boldsymbol{H}} - \hat{\boldsymbol{A}}) = 0 \tag{16}$$

Since both $\hat{\boldsymbol{H}}$ and $\hat{\boldsymbol{A}}$ are upper triangular matrices, (16) can be written as:

$$\det(\lambda\hat{\boldsymbol{H}} - \hat{\boldsymbol{A}}) = \prod_{i=1}^{l}(\lambda\hat{H}_{ii} - \hat{A}_{ii}) = 0$$

where $\hat{H}_{ii}$ and $\hat{A}_{ii}$: the i^{th} diagonal element of $\hat{\boldsymbol{H}}$ and $\hat{\boldsymbol{A}}$ respectively.

Therefore λ can be solved easily as:

$$\lambda_i = \hat{A}_{ii} / \hat{H}_{ii} \qquad (\text{if } \hat{H}_{ii} \neq 0) \tag{17}$$

Since $\widetilde{\boldsymbol{H}}$ is rank deficient for our case, we can assume $\widetilde{\boldsymbol{H}}$ in the format of:

$$\widetilde{\boldsymbol{H}} = \begin{bmatrix} \boldsymbol{I}_{n\times n} & \boldsymbol{0}_{n\times m} \\ \boldsymbol{0}_{m\times n} & \boldsymbol{\varepsilon}_{m\times m} \end{bmatrix}$$

where $\boldsymbol{\varepsilon} = \text{diag}\,(\varepsilon_1 \ldots \varepsilon_i \ldots \varepsilon_m)$; $\varepsilon_i >\approx 0$ ($i = 1, \ldots, m$): infinitesimal time constant in nature.

Then after Schur decomposition, there will be some diagonal elements $\hat{H}_{ii}$ of $\hat{\boldsymbol{H}}$ with extremely small values, which correspond to ε_i in $\widetilde{\boldsymbol{H}}$ and lead to infinite eigenvalue λ_i in (17). This can easily be identified as "fictitious" eigenvalues and spurned.

After true eigenvalue λ_i (i=1,…,n) calculation, its corresponding generalized right (left) eigenvector $\widetilde{\boldsymbol{e}}_i$ ($\widetilde{\boldsymbol{f}}_i$) can be calculated by:

$$\lambda_i \widetilde{\boldsymbol{H}}\widetilde{\boldsymbol{e}}_i = \widetilde{\boldsymbol{A}}\widetilde{\boldsymbol{e}}_i,\ \lambda_i \widetilde{\boldsymbol{H}}\widetilde{\boldsymbol{f}}_i = \widetilde{\boldsymbol{A}}^{\mathrm{T}}\widetilde{\boldsymbol{f}}_i \tag{18}$$

where $\widetilde{\boldsymbol{e}}_i = \begin{bmatrix} \boldsymbol{e}_i \\ \boldsymbol{e}'_i \end{bmatrix}$, $\widetilde{\boldsymbol{f}}_i = \begin{bmatrix} \boldsymbol{f}_i \\ \boldsymbol{f}'_i \end{bmatrix}$ (($\boldsymbol{e}_i$, $\boldsymbol{f}_i$) is defined in (10)). It is easy to prove:

$$\boldsymbol{e}'_i = -\boldsymbol{D}^{-1}\boldsymbol{C}\boldsymbol{e}_i,\quad \boldsymbol{f}'_i = -(\boldsymbol{B}\,\boldsymbol{D}^{-1})^{\mathrm{T}}\boldsymbol{f}_i$$

It is well known that ($\boldsymbol{e}_i$, $\boldsymbol{f}_i$) provides the information of observability and controllability of state variables $\boldsymbol{X}$ on mode λ_i. Similarly ($\boldsymbol{e}'_i$, $\boldsymbol{f}'_i$) provides the similar information of algebraic variables $\boldsymbol{Y}$ on mode λ_i. The information is very useful for designing controllers for SSO damping.

Generalized Schur decomposition can be used to apply the complete eigen-analysis based on the LDAE model directly. However, for very large power systems, the complete eigen-analysis is difficult to implement without system reduction. Alternatively, by taking advantages of power system sparsity, some iterative methods [10] are used to compute the system critical eigenvalues quickly also based on the LDAE model. These methods deserve the author to study furthermore on how to solve the torsional modes in large power systems.

Since the LDAE model preserves all algebraic variables and system structure, it is also very convenient to conduct eigenvalue sensitivity [11].

4 COMPLEX TORQUE COEFFICIENT CALCULATION BASED ON LDAE MODEL

The frequency-scanning CTC calculation is widely used for SSO study, which can provide CTC information over the entire subsynchronous frequency range and detect potential SSO risk. The CTC calculation formula can be derived from the suggested LDAE Model, which is given below.

4.1 Principle of CTC Calculation Based on LDAE Model

From SSO theory [9], we know that for a certain machine (here it is the studied machine), its spring-mass shaft model can be expressed as a torsional-mode-decoupled model (see figure 1) when mechanical damping is neglected. When a properly selected matrix is used to convert the multi-mass shaft model to modal-space with governor dynamics ignored (ΔT_{mi}=0), each modal-space mass experiences a common electromagnetic torque ΔT_e of the generator and the generator mass rotor angle $\Delta\delta_G$ has the relation: $\Delta\delta_G = \sum_{i=1}^{N} \Delta\delta_i^{(m)}$ (N: total number of masses on the shaft; superscript (m): modal space variable), i.e. (see figure 1):

$$\omega_B^{-1} M_i^{(m)} p^2 \Delta\delta_i^{(m)} + K_i^{(m)} \Delta\delta_i^{(m)} = -\Delta T_e \ (i = 1 \sim N),$$
$$\Delta\delta_G = \sum_{i=1}^{N} \Delta\delta_i^{(m)} \tag{19}$$

where $M_i^{(m)}$: modal inertial constant (in sec) of the *i-th* shaft mode; $K_i^{(m)}$: modal spring constant (in pu torque/rad) of the *i-th* shaft mode; ΔT_e: in pu; ω_B: the system frequency base in rad/sec; rotating mass angle ($\Delta\delta_G$ or $\Delta\delta_i^{(m)}$): in rad; $p = d/dt$ with t in sec.

It is clear from (19) and figure 1 that only $\Delta\delta_G$ and ΔT_e of the studied machine will interface the shaft model in modal-space to the remaining system, and the latter can be seen as a SISO system with input $\Delta\delta_G$, output ΔT_e and apparent overall transfer function of $G(p)$.

Based on above analysis and figure 1, CTC of the studied machine can be worked out easily based on the suggested LDAE model. It should be noticed that the transfer function of $G(p)$ has included the effects of other machine shaft dynamics, all machine electric circuit transients (with exciter effects included) and other elements and network transients accurately.

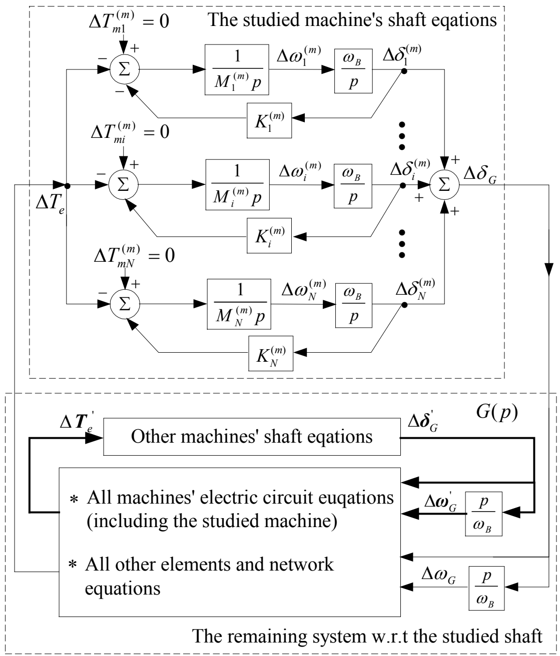

Figure 1: CTC calculation based on LDAE model

4.2 Procedure of CTC Calculation

The procedure of calculating the electrical CTC of the studied machine based on LDAE model is as follows.

(i) Taking off the spring-mass shaft equations (3) of the studied machine from (8), we can get (keep the differential operator $p = d/dt$, t in sec):

$$\begin{bmatrix} p\boldsymbol{X}' \\ \boldsymbol{0} \end{bmatrix} = \begin{bmatrix} \boldsymbol{0} & \boldsymbol{A}'_{\omega} & \boldsymbol{A}' & \boldsymbol{B}' \\ \boldsymbol{C}'_{\delta} & \boldsymbol{0} & \boldsymbol{C}' & \boldsymbol{D}' \end{bmatrix} \begin{bmatrix} \Delta\delta_G \\ \Delta\omega_G \\ \boldsymbol{X}' \\ \boldsymbol{Y} \end{bmatrix} \tag{20}$$

where $\boldsymbol{X}'$:subset-vector of state variables $\boldsymbol{X}$ exclusive $\boldsymbol{X_S}$ of the studied machine.

$\Delta\delta_G$ (in rad) and $\Delta\omega_G$ (in p.u.) are the angle and speed increments of generator-mass of the studied machine, which act as the 'input signal' to the 'remaining system' as mentioned above. It should be noticed that electromagnetic toque algebraic equation (4) is kept in the system model, which is included in (20).

(ii) $\Delta\delta_G$ and $\Delta\omega_G$ should satisfy the relation $\Delta\omega_G = \frac{1}{\omega_B} p\Delta\delta_G$ (where ω_B is the system frequency base in rad/sec), hence we can simplify (20) further and obtain:

$$\begin{bmatrix} p\boldsymbol{X}' \\ \boldsymbol{0} \end{bmatrix} = \begin{bmatrix} \frac{p}{\omega_B}\boldsymbol{A}'_\omega & \boldsymbol{A}' & \boldsymbol{B}' \\ \boldsymbol{C}'_\delta & \boldsymbol{C}' & \boldsymbol{D}' \end{bmatrix} \begin{bmatrix} \Delta\delta_G \\ \boldsymbol{X}' \\ \boldsymbol{Y} \end{bmatrix}$$

(iii) Rearrange above equation to:

$$\begin{bmatrix} \boldsymbol{A}' - p\boldsymbol{I} & \boldsymbol{B}' \\ \boldsymbol{C}' & \boldsymbol{D}' \end{bmatrix} \begin{bmatrix} \boldsymbol{X}' \\ \boldsymbol{Y} \end{bmatrix} = -\begin{bmatrix} \frac{p}{\omega_B}\boldsymbol{A}'_\omega \\ \boldsymbol{C}'_\delta \end{bmatrix} \Delta\delta_G \qquad (21)$$

Thus we can consider that $\boldsymbol{X}'$ and $\boldsymbol{Y}$ are implicit linear functions of $\Delta\delta_G$ including operator p and denote them to:

$$\boldsymbol{X}' = \boldsymbol{K}_X(p)\Delta\delta_G\,,\quad \boldsymbol{Y} = \boldsymbol{K}_Y(p)\Delta\delta_G \qquad (22)$$

(iv) Set $p = j\Omega$ in (21) (where Ω is a certain frequency of interest in rad/sec within subsynchronous frequency band). If we have moved the element $\boldsymbol{Y}_{Te}$ (corresponding to the electromagnetic torque ΔT_e of the studied machine) relevant equation to the last equation in (21), it is easy to solve for it as $\Delta\delta_G$'s function through only forward Gaussian elimination of (21), and the obtained complex coefficient in (23) is the required CTC.

$$\left.\frac{\Delta T_e}{\Delta\delta_G}\right|_{p=j\Omega} = K_e(\Omega) + j\frac{\Omega}{\omega_B} D_e(\Omega) \qquad (23)$$

where K_e: electrical synchronizing torque coefficient; D_e: electrical damping torque coefficient. Sparse matrix technique can be applied in CTC calculation.

The electrical damping torque coefficient D_e varies with system topology, parameter and the operation point. For complicated power systems with HVDC transmission and/or FACTS devices, the value of D_e includes their impacts as well.

4.3 Stability Judgement for Torsional Mode

Based on section 4.1 and (19), if we assume that the mechanical damping of the *i-th* modal $D_i^{(m)}$ is already known (say determined from decrement tests or some other methods), we can make stability judgement for the *i-th* torsional mode of frequency Ω based on $D_i^{(m)}$ and calculated $D_e(\Omega)$ according to the following rules:

- If $D_i^{(m)} + D_e = 0$, the torsional mode is critical.
- If $D_i^{(m)} + D_e > 0$, the torsional mode is stable.
- If $D_i^{(m)} + D_e < 0$, the torsional mode is unstable.

In this paper, the method suggested in [12] is adopted to calculate modal mechanical damping torque coefficients approximately. The eigenvalues of the studied spring-mass shaft alone are calculated first (i.e. eigenvalues for equation (3) with $\boldsymbol{Y}_{Te} = 0$). Then modal mechanical damping coefficient can be calculated by: $D_i^{(m)} \approx -2\sigma_i M_i^{(m)}$, where σ_i is Re(λ_i) of the *i-th* mode λ_i.

We also assume that (i) after connecting to the system, the real torsional oscillation frequency (Ω) is close to its natural frequency $\omega_i^{(m)}$, which is known prior to CTC calculation; and (ii) the modal interaction among different torsional modes of the studied machine can be neglected so that each time we can study only one particular torsional mode.

Some remarks are presented as follows.

(i) If we assume the torsional frequency is unchanged after connecting the torsional shaft system with the remaining system, that means we can simply use D_e (calculated from (23)) at $\Omega \approx \omega_i^{(m)}$ to judge the stability of the *i-th* torsional mode. The rate of divergence (or decay) of the torsional oscillation can be approximately weighed by the value of $-(D_i^{(m)} + D_e(\Omega))/(2M_i^{(m)})$ (where $M_i^{(m)}$ is the modal inertia constant).

(ii) However, the frequency of the torsional mode will actually deviate from its natural frequency to small extent with impacts on real K_e and D_e. Hence, when studying the *i-th* torsional mode, we can assume the maximum frequency shift is ζ_i rad/sec. Then we can check the value of $D_i^{(m)} + D_e$ within the frequency band $\Omega \in (\omega_i^{(m)} - \zeta_i,\ \omega_i^{(m)} + \zeta_i)$, if $D_i^{(m)} + D_e$ is always negative (positive), the torsional mode is unstable (stable). Whereas if $D_i^{(m)} + D_e$ changes its polarity more than once within the studied frequency band, we can not absolutely confirm the stability of the torsional mode.

(iii) The system is assumed to be stable if composite damping torques ($D_i^{(m)} + D_e$) within the vicinity of all shaft torsional frequencies are positive.

(iv) Although CTC analysis method is not as accurate as eigen-analysis or time simulation, we must admit that it is still an effective way to predict the stability of the torsional modes. Especially it can be applied in SSO study for very large-scale power systems with HVDC or/and FACTS when eigen-value and time simulation are difficult to apply without system reduction.

5 COMPUTER STUDY RESULTS

A two-machine-infinite-bus power system is used for test (see figure 2). The system data is given in appendix. The shaft of G1 is taken from the IEEE FBM and the shaft of G2 has four masses. The modal-space shaft parameters are listed in table 1 before connecting generators to the system. Under the condition of series capacitor compensating 80% of the line reactance and G1 and G2 are connected to the system with the power output of 600MW and 520MW respectively, computer tests are conducted.

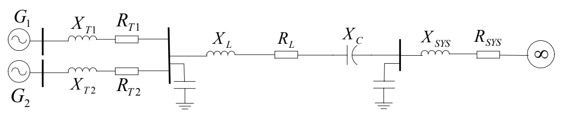

Figure 2: Two-machine-infinite-bus power system one-line diagram

Torsional Mode		$\omega_i^{(m)}$ (rad/sec)	$f_i^{(m)}$ (Hz)	$M_i^{(m)}$ (sec)	$K_i^{(m)}$ (pu/rad)	$D_i^{(m)}$ (pu)
G1	1	98.72	15.71	5.402	139.65	0.159
	2	126.95	20.20	55.4	2368.4	7.282
	3	160.52	25.55	13.838	945.77	0.461
	4	202.85	32.28	7.845	856.25	0.066
	5	298.18	47.46	22577	5324446	820.84
G2	1	135.24	21.52	4.479	217.29	0.078
	2	193.80	30.84	6.637	661.28	0.090
	3	266.80	42.46	433.26	81806	12.290

Table 1: Modal quantities of shaft systems of G1 & G2

Generalized eigen-analysis based on LDAE model is performed after the generators connect to the system with test results given in table 2. From table 2 we can see that the torsional modes λ_1^{G1} and λ_3^{G1} of G1 are unstable, and the torsional mode λ_1^{G2} of G2 is unstable as well. In addition, when comparing torsional mode oscillation frequencies shown in table 1 ($\omega_i^{(m)}$) and table 2 (Im(λ_i)), we can see that after connecting to the system the shaft torsional frequency shift from their original natural oscillation frequencies is very small.

Torsional Mode		Re(λ_i)=σ_i (1/sec)	Im(λ_i) =ω_i (rad/sec)	f_i=ω_i/2π (Hz)
G1	λ_1^{G1}	0. 04883	99.59	15.85
	λ_2^{G1}	-0. 03324	127.04	20.22
	λ_3^{G1}	0.04039	160.54	25.55
	λ_4^{G1}	-0.00158	202.99	32.31
	λ_5^{G1}	-0.01818	298.18	47.46
G2	λ_1^{G2}	0. 29845	135.87	21.62
	λ_2^{G2}	-0. 00555	193.99	30.87
	λ_3^{G2}	-0.01418	266.80	42.46

Table 2: Eigen-analysis results

At the same operation point, the proposed LDAE-model-based CTC calculation is also conducted and compared with eigen-analysis results. The calculated K_e and D_e of G1 & G2 w.r.t scanning frequency Ω are shown in figures 3 (a) & (b) respectively (only the frequency range of 90~190 rad/sec is plotted since the damping torque coefficient D_e remains to be close to 0 over the ranges of 0~90 and 90~ω_B rad/sec). The three vertical dash-dot lines from left to right in figure 3 (a) correspond to the natural frequencies of torsional modes 1, 2 & 3 of G1 respectively, and the one vertical dash-dot line in figure 3 (b) corresponds to the natural frequency of torsional mode 1 of G2. The torsional stability of G1 will be discussed first. It can be observed from figure 3 (a) that in the vicinities of torsional modes 1, 2 & 3 of G1, the system exhibits all negative electric damping (D_e < 0), which assumes that the torsional modes 1, 2 & 3 of G1 are potential candidates of unstable modes. However, the conclusion has to be made after comparing D_e(Ω) with the modal-space mechanical damping torque coefficient $D_i^{(m)}$. As to the torsional stability of G2, it can be seen from figure 3 (b) in the vicinities of torsional modes 1 of G2, the system exhibits clearly negative electric damping D_e. Hence, torsional mode 1 of G2 is the potential candidate of unstable mode.

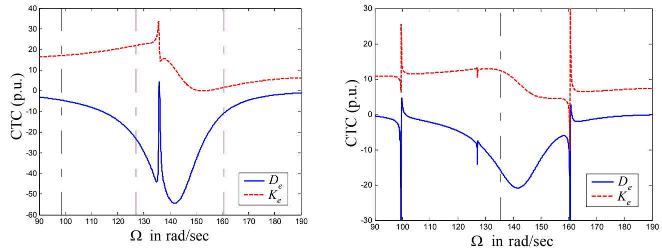

(a) CTC of G1

(b) CTC of G2

Figure 3: CTC calculation results

It should be noticed that when calculating the CTC of G1, both K_e and D_e will have drastic change at the torsional oscillation frequencies of G2 and vice versa. If the torsional oscillation frequencies of G1 and G2 are not close to each other, it is feasible to judge one machine's torsional stability according to its CTC calculation results. However, when any torsional oscillation frequencies of G1 and G2 are very close to each other, it will be difficult to judge the stability of corresponding mode only through CTC calculation.

Torsional Mode		$D_i^{(m)}$ (pu) M Base	$D_i^{(m)}$ (pu) S Base	D_e (pu) Ω in $\omega_i^{(m)}$ S base	$-\frac{D_i^{(m)}+D_e}{2M_i^{(m)}}$ (1/sec)
G1	1	0.159	1.113	-4.5834	0.04589
	2	7.282	50.974	-23.102	-0.03594
	3	0.461	3.227	-11.099	0.04063
	4	0.066	0.462	-0.2842	-0.00162
	5	820.84	5745.9	-0.0521	-0.01818
G2	1	0.078	0.468	-15.827	0.28576
	2	0.090	0.540	-0.0941	-0.00560
	3	12.290	73.740	0.00152	-0.01418

Table 3: Numerical results of CTC information

The composite effects of $D_i^{(m)}$ and D_e(Ω) are given in table 3. All $D_i^{(m)}$ and D_e(Ω), including inertial constants $M_i^{(m)}$ have been referred to the common system base of 100 MVA. From table 3 we can see that ($D_i^{(m)}$+ D_e(Ω)) of torsional modes 1 & 3 of G1 are negative, hence these modes are unstable. Whereas torsional mode 2 of G1is actually stable because of its positive ($D_i^{(m)}$ + D_e (Ω)). And torsional mode 1 of G2 is unstable. Furthermore, when comparing $-\frac{D_i^{(m)}+D_e}{2M_i^{(m)}}$ (approximate decay coefficient) in table 3 w.r.t Re(λ_i) in table 2, it can be observed that for torsional modes 1~5 of G1 and torsional modes 2~3 of G2 with relatively smaller |Re(λ_i)|, the decay coefficients obtained through CTC calculation method and eigen-analysis are quite close to each other. For torsional mode 1 of G2 with relatively bigger |Re(λ_i)|, still the stability judgement via CTC calculation is consistent to the eigen-analysis. Although the decay coefficient has a relatively larger deviation from that of eigen-analysis, it is within 5%. Actually using "complex frequency scanning" and iteration, more accurate decay coefficient can be obtained for mode 1 of G2 at the cost of CPU time as tested by the authors.

6 CONCLUSION

In this paper, a LDAE model for power system SSO study is proposed. The system LDAE model can be established efficiently through two steps with element LDAE models as building blocks. Generalized eigen-analysis can be directly applied to the LDAE model for SSO study. The results can provide useful information of observability and controllability of algebraic variables on individual SSO modes. Furthermore, the frequency-scanning CTC calculation can be easily realized based on the LDAE model, which is useful for stability judgement of torsional modes. The computer test results show clearly the effectiveness of the proposed LDAE model and the relevant analysis. The CTC calculation results are compared favorably with that from the generalized eigen-analysis. The LDAE-based SSO study model and its corresponding analysis methods pave the way to include HVDC transmission and FACTS device models in SSO study and get deep insight about their effects on SSO.

ACKNOWLEDGMENT

The research is supported by NSF of China (No. 50337010), National Key Basic Research Special Fund, P.R. China (2004CB217900), and RGC of Hong Kong Government, to whom the authors would like to express their sincere acknowledgements.

APPENDIX

The two-machine-infinite-bus power system data is as follows.

The generator data (pu on machine MVA base, time constants in sec.)

G1 (rated MVA=700, rated kV=22.0) data:

$r_a = 0.001, l_a = 0.13, L_d = 1.79, L_d^{'} = 0.169, L_d^{''} = 0.135,$

$L_q = 1.71, L_q^{'} = 0.228, L_q^{''} = 0.20$.

$\tau_{d0}^{'} = 4.30, \tau_{d0}^{''} = 0.032, \tau_{q0}^{'} = 0.85, \tau_{q0}^{''} = 0.050$

G2 (rated MVA=600, rated kV=22.0) data:

$r_a = 0.0045, l_a = 0.14, L_d = 1.65, L_d^{'} = 0.25, L_d^{''} = 0.20,$

$L_q = 1.59, L_q^{'} = 0.46, L_q^{''} = 0.20$.

$\tau_{d0}^{'} = 4.50, \tau_{d0}^{''} = 0.040, \tau_{q0}^{'} = 0.55, \tau_{q0}^{''} = 0.090$

Spring-mass shaft data

G1: same as IEEE FBM model [13] (self-damping constant of each mass is supposed to be 0.01 pu with mutual damping between adjacent masses neglected).

G2: a four-mass shaft with its shaft data as follows (pu on machine MVA base):

Inertial constants (in sec):

$M_{Gen} = 0.8785, M_{LP} = 1.2235, M_{IP} = 0.4263, M_{HP} = 0.1101.$

Spring constants (in pu):

$K_{Gen-LP} = 81.852, K_{LP-IP} = 60.358, K_{IP-HP} = 28.255.$

Self-damping constants in pu (mutual damping between adjacent masses is neglected):

$D_{Gen} = D_{LP} = D_{IP} = D_{HP} = 0.01$.

The network impedance (pu value on 100 MVA base)

$R_{T1} = 0.0002, X_{T1} = 0.02, R_{T2} = 0.0004, X_{T2} = 0.04,$

$R_L = 0.0052, X_L = 0.054, R_{SYS} = 0.0014, X_{SYS} = 0.03$.

REFERENCES

[1] IEEE Committee. "The 4th Supplement to a Bibliography for SSR", IEEE Trans. On PWRS, 1997

[2] N.Rostamkolai, R.J.Piwko, et al. Subsynchronous Torsional Interactions with Static VAR Compensators Influence of HVDC. IEEE Trans. On Power Systems, 1991, 6(1):255 – 261.

[3] Pilotto, L.A.S.; Bianco, A.; Long, W.F.; Edris, A.-A.; Impact of TCSC Control Methodologies on Subsynchronous Oscillations. IEEE Trans. On Power Delivery, 2003, 18(1):243 – 252

[4] Wan Bo, Zhang Yan, "Damping subsynchronous oscillation using UPFC-a FACTS device", Power System Technology, 2002. Proceedings. PowerCon 2002. International Conference on , Volume: 4 , 13-17 Oct. 2002 Pages:2298 - 2301 vol.4

[5] IEEE Committee. "Reader's Guide to Subsynchronous Resonance", IEEE Trans. On Power Systems, 1992, 7(1):150 – 157

[6] IEEE Committee Report, "Comparison of SSR Calculations and Test Results", IEEE Trans. On Power Systems, Vol. 4, No. 1, pp. 336-344, February 1989.7

[7] Canay I. M., "A Novel Approach to the Torsional Interactions and Electrical Damping of the Synchronous Machine, Part-I: Theory, Part-II: Application to an arbitrary network", IEEE Transactions on Power Apparatus and Systems, Vol. PAS-101, No.10, pp. 3630-3640, 1982

[8] Anderson, E., Z. Bai, C. Bischof, S. Blackford, J. Demmel, J. Dongarra, J. Du Croz, A. Greenbaum, S. Hammarling, A. Mckenney, and D. Sorensen, "LAPACK User's Guide", Third Edition, SIAM, Philadelphia, 1999

[9] P. M. Anderson, B. L. Agrawal, J. E. Van Ness. Subsynchronous Resonance in Power Systems, IEEE Press, New York, 1990

[10] Improved methodologies for the calculation of critical eigenvalues in small signal stability analysis, Angelidis, G.; Semlyen, A.; IEEE Transactions on Power Systems, Volume 11, Issue 3, Aug. 1996 Page(s):1209 – 1217

[11] Feasible eigenvalue sensitivity for large power systems, Smed, T.; IEEE Transactions on Power Systems, Volume 8, Issue 2, May 1993 Page(s):555 - 563

[12] T. Hara, N. Kobayashi, "Development of A Damping Analysis Program for Multi-Generator Power Systems", IEEE Transactions on Power Systems, Vol. 9, No. 4: 1803 – 1810.

[13] IEEE SSR Working Group. "First Benchmark Model for Computer Simulation of SSR", IEEE Trans. On PAS, 1977, 96(5): 1565 – 1572